*International Journal of the Korean Society of Precision Engineering Vol. 3, No. 3, July 2002.*

# Dynamic Fracture Toughness of Chevron-notch Ceramic Specimens measured in Split Hopkinson Pressure Bar

Yeon-Soo Lee[1], Young-Ki Yoon[2], and Hi-Seak Yoon[3]

[1] Department of Orthopaedic Surgery, VA Healthcare System and University of California in Irvine, USA
[2] School of Mechanical & Aerospace Engineering, Seoul National University, KOREA
[3] School of Automotive Engineering, Chonnam National University, KOREA

## ABSTRACT

Measuring dynamic fracture toughness of brittle and small ceramic specimen is very difficult in a SHPB (Split Hopkinson Pressure Bar). As a countermeasure to this difficulty, a dynamic fracture toughness measuring method by the Chevron-notch ceramic specimen was proposed. Tested chevron specimens were of Chevron notch angles of 90°, 100° and 110°. Through finite element analysis, shape parameters of the Chevron-notch specimens according to notch angles were calculated. And the static fracture toughness of the Chevron-notch alumina specimen was measured as 3.8 $MPa\sqrt{m}$ similar to that of CT specimen with a precrack. Dynamic fracture toughness was 4.5 $MPa\sqrt{m}$ slightly higher than the static one. It was shown in this study that the proposed Chevron-notch specimens are valid to measure dynamic fracture toughness of extremely brittle materials such as ceramic.

**Key Words :** The split Hopkinson pressure bar (SHPB), dynamic fracture toughness, Chevron notch, FEA, dimensionless stress intensity factor

### Nomenclature

$P_{max}$ = Maximum tensile load
$K_{IC}$ = Static fracture toughness
$K_{IvM}$ = Static fracture toughness of Chevron-notch specimen determined by $P_{max}$
$Y$ = Dimensionless stress intensity factor

## 1. Introdution

Though ceramic material has been widely used as a thermal barrier owing to its thermal cut-off property, its brittleness and low toughness have brought limitation in its application. Many researches have been carried out to promote its brittleness and to evaluate the fracture toughness of ceramic materials.

However, more reliable method to measure the fracture toughness must be established. Since mechanical machining of a ceramic specimen is not easy, the use of Chevron-notch specimens have been increasing. To make a sharp precrack in a specimen made of glass or of ceramic, R.W. Davidge and G. Tappin[1] applied a bending load parallel to the specimen's section together with a compressive load along the longitudinal direction. But this method is tedious and time-comsuming and also can not insure consistency in the notch shape of specimens.

Miyahara et. al.[2] evaluated the usefulness of several static fracture toughness measuring methods. In their study, FP method (fatigue pre-cracking from the crack introduced by BC method), CSF method (controlled surface flow method) and CN method (Chevron-notch method) were found to be adequate for measuring the fracture toughness of brittle materials. But BC method (bridge compression method) and IF method (indentation fracture method) were concluded as being not suitable.

ASTM E1304[3], a test standard of CN method,

mentions that fracture toughness can be obtained using a Chevron-notch specimen made of brittle material such as high-strength aluminum alloy and using measured compliance from a tensile test. And if a mateial shows a constant crack resistance curve, the fracture toughness of the material is determined only by measuring the maximum tensile load[4]. Because crack propagation in a very brittle material suddenly turns out to be unstable, making a precrack by fatigue loads would be a very difficult job. But, ceramic materials or brittle metals having uniform microstructure show a constant crack resistance after some amount of the crack growth. Thereby, if we use the Chevron-notch specimen showing a concave crack driving force under a constant load, its fracture toughness could be determined only by the maximum tensile load[5].

The dynamic fracture properties of a material have been widely studied using SHPB (Split Hopkinson Pressure Bar). But, SHPB method has limitations in the size and the shape of the specimen due to the size and the configuration of SHPB. Specially for the specimen made of brittle material, making a precrack is very difficult unless the size of the specimen is large. Chen and Ravichandran[5] studied dynamic fracture behaviors of a ceramic specimen with a shrink-fit metal sleeve by inspecting the fractured section from SHPB tests. Anton and Subhash[6] measured a Vickers hardness using the dynamic indentation hardness measurement method based on ASTM C1327. And they calculated the dynamic fracture toughness using Lankford's $K_{IC}$ estimation[11]. As mentioned in the work of Miyahara et. al.[2], the upper two methods are inadequate. On the contrary, the usefulness of Chevron notch method to measure static fracture toughness has been supported by several reports quoted above and by ASTM E1304.

Until now, nevertheless, there are little successful researches on measuring dynamic fracture toughness using Chevron notch in SHPB. And there is not any authorized standard testing regulation about CN method in the SHPB test. Due to these reasons, a method to measure the dynamic fracture toughness in SHPB apparatus was tried by adopting a Chevron notch specimen made of alumina ($Al_2O_3$-99.5%). Using specimens with different Chevron notch angles, the optimal shape of Chevron-notch specimen for measuring dynamic fracture toughness was also studied.

Generally the static fracture toughness of alumina is known to be about 4 $MPa\sqrt{m}$ [7]. For a Chevron-notch specimen of 90°, the static fracture toughness was 3.84 $MPa\sqrt{m}$ and the dynamic one from SHPB test was 4.50 $MPa\sqrt{m}$. . The specimens of 100° showed slightly smaller value but similar trend. But for the specimens of 110°, the measured values were thought to be invalid because those were too low due to unstable crack propagation. Because of inertia effect in a dynamic mode, dynamic fracture toughness is slightly higher than static one. Also in these tests, the measured values of dynamic fracture toughness were 17~20% higher than static ones.

## 2. Experiments

### 2.1 Tensile Chevron-notch Specimen

Fig. 1 illustrates the shape of the proposed Chevron-notch specimen where L is the length of the specimen, θ is a Chevron notch angle and t is the thickness of a notch groove. And, α is a relative crack length expressed as Eq. (1).

$$\alpha = a/D \tag{1}$$

If a specimen behaves linear elastically, the static fracture toughness ( $K_{IC}$) of a Chevron-notch specimen is determined by the maximum fracture load ( $P_{max}$ ) and is denoted by $K_{IvM}$ (ref. ASTM E1304).

$$K_{IvM} = \frac{P_{max}}{D^{3/2}} Y_c \tag{2}$$

In Eq. (2), $Y_c$ is a minimum dimensionless stress intensity factor which is charactered by geometrical values such as crack length a and width of the notch D.

Since the alumina is a very brittle material, the specimens were machined into dog-bone shape and had three kinds of Chevron notch angles as 90 ◦ , 100 ◦ and 110 ◦ as seen in Fig. 2 and 3. A Chevron notch was made in the gage length, which is in the middle part of the specimen and has a uniform diameter. The total length, the diameter and the gage length of the specimen were 48.7mm, 5mm and 12.7mm, respectively. The specimens were designed to be used in both static tensile and SHPB tests. Because machining of a screw for a brittle ceramic specimen is very difficult, the dog-bone specimen was fixed by using screw jigs and screw-jointed

to a loading fixture as shown in Fig. 4.

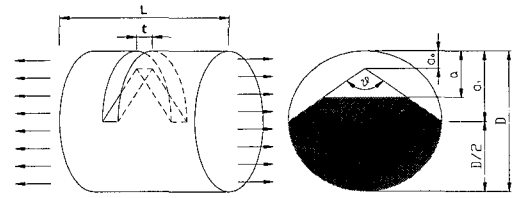


Fig. 1 Schematic diagram of chevron notched specimen newly proposed in this study

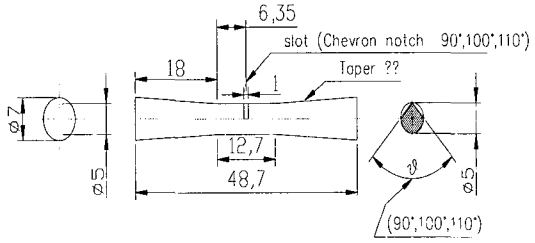


Fig. 2 Demensions of tensile specimen (in mm)

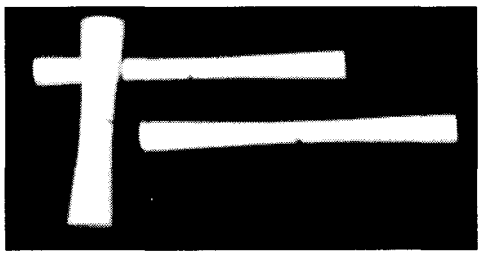

Fig. 3 Photography of ceramic specimensimens with a chevron notch

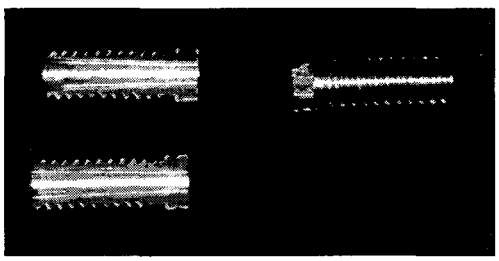

Fig. 4 Screw jigs to hold a ceramic specimen

### 2.2 Static tensile tests

Static tensile specimens were also made from the alumina. Static tensile tests were performed to get the maximum tensile strength which would be used to determine the Mode I fracture toughness of Chevron-notch specimen. The tensile tests were done with INSTRON universal tester under the displacement speed of 0.01mm/sec.

When a specimen and screw jigs are installed in the loading fixtures of tensile tester, the loading center could be misaligned. In that case, misaligned center may cause the fracture of specimen at the installation stage of specimen or abnormally low tensile fracture load of specimen. To prevent these problems, a set of universal joints were used.

### 2.3 SHPB Test

Fig. 5 shows a schematic diagram of SHPB apparatus. Three main bars composing the SHPB tester are striker bar, input bar and output bar. The three bars are made of Inconel 718 and have lengths of 25cm, 150cm and 75cm, respectively. Strain pulses are detected in the strain gages A and B that are located in the same distance from the installation position of specimen

Fig. 6 shows the detail sketch of ceramic specimen installed in the SHPB apparatus. A specimen was installed between the input and the output bars. To introduce a tensile load to the specimen, a hollow collar was inserted between the bars. The collar covers the specimen without any contact. A compressive wave from the input bar is transmitted to the output bar without any effect on the specimen. And this compressive wave reflects at the right end of the output bar and becomes a tensile wave which is applied to the specimen.

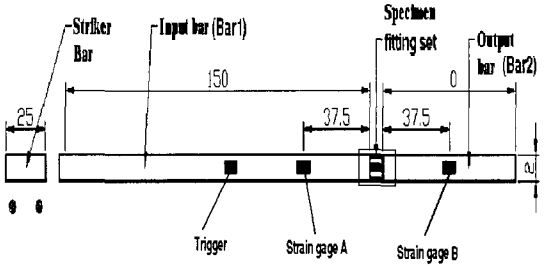


Fig. 5 Schematic diagram of SHPB apparatus (Dimensions are in *cm*)

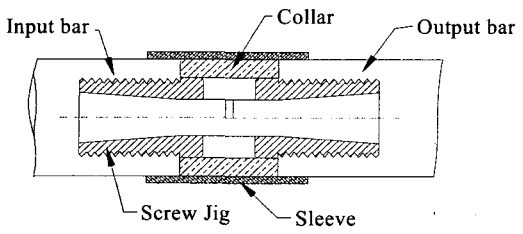


Fig. 6 Detail sketch of ceramic specimen installed between the bars in SHPB

## 3. Finite Eilement Analysis

In general, there are two methods to determine the dimensionless stress intensity factor which depends on the geometrical shape. One is so-called the compliance method by experiment and the other is the finite element method(FEM) by numerical analysis. In this study, we used the finite element analysis method.

Fig. 7 shows the finite element model. The diameter and the length of the model are 5mm and 12.7mm, respectively. The Chevron notch angles of the model were 90°, 100° and 110°. The 20-node iso-parametric brick elements were used for the most parts and 16-node wedge elements for the crack tip. To impose a singularity to the crack tip, the middle nodes on the edges of elements crossing the crack tip were moved 1/4 length of the edge toward the crack tip[9,10](Fig. 8).

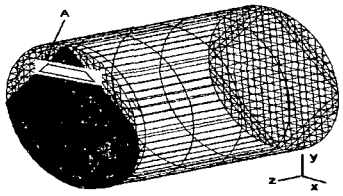

Fig. 7 FEM Model corresponding to the gage length of a Chevron-notch specimen

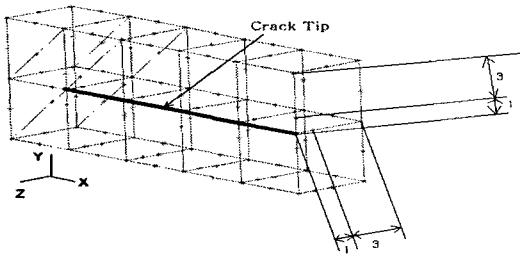


Fig. 8 FE modeling of crack tip singularity

The finite element model was solved linear elastically with ABAQUS V5.8. Table 1 lists the material properties of alumina ( $Al_2O_3$) used for the finite element analysis (2).

Table 1. Properties of alumina(99.5% $Al_2O_3$)

| $Al_2O_3$ | Young's modulus(E) | Poisson's ratio(υ) | Density(ρ) |
|---|---|---|---|
| | 343 GPa | 0.23 | 3.90 g/㎤ |

## 4. Results

### 4.1 Results of Finite Element Analysis

Fig. 9 shows the load-displacement curve according to the crack length obtained from FEM analysis of the specimen with Chevron notch angle of 90°. The four lines in Fig. 9 represents the load-displacement data at four steps of relative crack length, respectively. Fig. 10 shows the variation of compliance in terms of relative crack length where CED is the dimensionless compliance defined as equation (3).

$$CED = C \times E \times D \tag{3}$$

where C, E and D mean compliance, Young's modulus and diameter of specimen, respectively.

The compliance (C) at relative crack length can be obtained by reversing the gradient of load versus displacement line in Fig. 9. The thin line in Fig. 10 shows linear interpolation and the thicker one is parabolic curve of the linear line. Parabolic equations of CED can be expressed as Eqs. 4-a, b and c for the specimens with Chevron notch angles of 90°, 100°and 110°, respectively.

$$CED_{(\theta=90°)} = 21.454\alpha^3 - 9.3611\alpha^2 + 2.053\alpha + 1.3585$$
$$CED_{(\theta=100°)} = 68.336\alpha^3 - 30.921\alpha^2 + 8.6368\alpha - 0.0454$$
$$CED_{(\theta=110°)} = 29.223\alpha^3 - 19.003\alpha^2 + 4.8485\alpha + 1.0275$$
(4-a) ~ (4-c)

Using the CED equations, dimensionless stress intensity factor (Y) could be calculated by the equation (2). Dimensionless stress intensity factor of the specimen with notch angle of 90° is displayed in Fig. 11. A thick curve is a 3rd order polynomial expression of four dimensionless stress intensity factors according to the

crack length. Dimensionless intensity factors for three types of Chevron notch angles are expressed as equations (5-a, 5-b and 5-c).

$$Y_{(\theta=90°)} = -105.09\alpha^3 + 97.974\alpha^2 - 25.893\alpha + 3.1485$$
$$Y_{(\theta=100°)} = -112.83\alpha^3 + 109.98\alpha^2 - 31.196\alpha + 3.9118$$
$$Y_{(\theta=110°)} = -153.37\alpha^3 + 169.52\alpha^2 - 58.1581\alpha + 7.5736$$
(5-a)~(5-c)

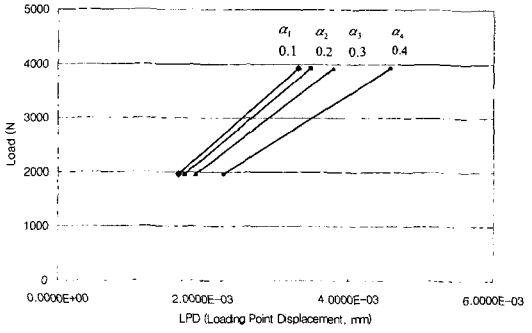


Fig. 9 Load-displacement diagram vs. crack length (notch angle=90°)

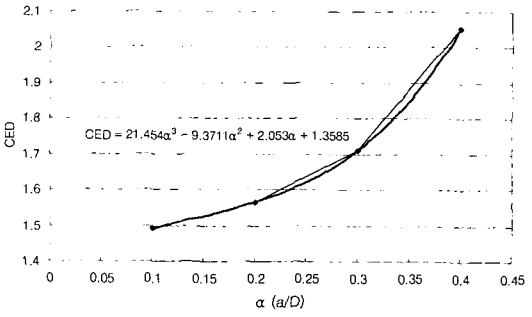


Fig. 10 Variation of dimensionless compliance vs. crack length (notch angle=90°)

Finally, minimum dimensionless stress intensity factor ( $Y_c$) was obtained by differentiating the 3rd order polynomial expressions of (5-a)~(5-c). The minimum value of dimensionless stress intensity factor for the specimen with notch angle of 90° was 1.04 around the relative crack length of 0.2.

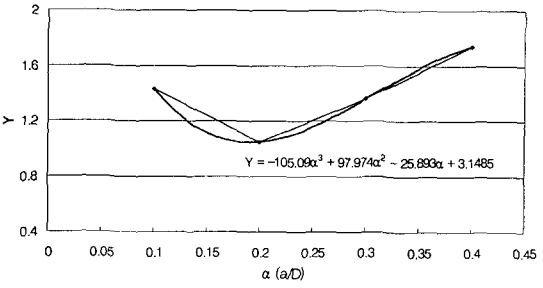


Fig. 11 Variation of dimensionless SIF vs. crack length (notch angle=90°)

## 4.2 Impact Stress Wave in SHPB

Fig. 12 shows strain signals from gages A and B for the specimen with Chevron notch angle of 90° and with striker bar velocity ( $v_o$) of 4.76 m/sec. In Fig. 12, the tensile stress wave ( $\varepsilon_T$) passed through the specimen is shown within a discontinuous circle, which was detected by the strain gage A after about 900 $\mu$sec. The small value of stress wave means that the ceramic material is easily fractured by a very small impact.

Table 2 lists the results from static and SHPB fracture tests of Chevron-notch specimens. Dynamic fracture loads from SHPB tests were 10~20% higher than static ones. Dynamic fracture load of a linear elastic material is generally higher than static one[8]. However, the fracture load of the specimen with notch angle of 110° was abnormally too low. If the notch angle is large, the area of fractured section changes rapidly. The initial crack length of 110° is larger than those of 90° and 100°. Hence, the variation of stress concentration becomes bigger as the crack propagates. Hence, steep change of section area gives rise to an unstable crack propagation and a lower fracture load.

Generally the static fracture toughness of alumina is known about 4 $MPa\sqrt{m}$ [7]. For a Chevron-notch specimen of 90°, the static fracture toughness was 3.84 $MPa\sqrt{m}$ and the dynamic one from SHPB test was 4.50 $MPa\sqrt{m}$ . The specimens of 100° showed slightly smaller value but similar trend. But for the specimens of 110°, the measured values were thought to be invalid because those were too low due to unstable crack propagation. Because of inertia effect in a dynamic mode, dynamic fracture toughness is slightly higher than static one. Also in these tests, the measured values of dynamic

fracture toughness were 17~20% higher than static ones.

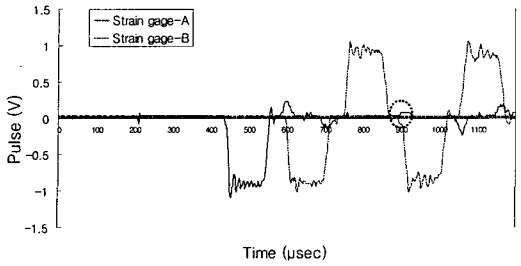


Fig. 12 Strain pulses detected in strain gages A and B for a ceramic specimen with a notch angle of 90° when striker bar velocity ( $v_o$) is 4.76m/sec

Table 2 A comparison of static and dynamic fracture loads for the alumina specimen

(N/A : Not available data)

| Chevron notch angle | | 90° | 100° | 110° |
|---|---|---|---|---|
| $P_s(N)$ | | 1305 | 1065 | 869 |
| $P_D(N)$ | | 1530 | 1276 | 956 |
| $Y_c$ | | 1.04 | 1.2 | 1.22 |
| $K_{IvM}$ ( $MPa\sqrt{m}$) | Static | 3.84 | 3.61 | 2.99(N/A) |
| | Dynamic | 4.50 | 4.33 | 3.29(N/A) |

## 5. Conclusion

In this study, authors proposed the Chevron-notch tensile specimens by which the measurement of dynamic fracture toughness can be possible in the crack opening mode. Its compatibility as a dynamic tensile fracture specimen was verified on Split Hopkinson Pressure Bar (SHPB) apparatus. Main results are as follows.

1) The static fracture toughness of alumina ( $Al_2O_3$) specimen with a Chevron notch of 90° was 3.8 $MPa\sqrt{m}$ and the dynamic one from the SHPB test was 4.5 $MPa\sqrt{m}$ . The specimens of 100° showed slightly smaller value but similar trend. And the specimens of 110° were judged inappropriate for the dynamic fracture specimen due to its unstable crack propagation.

2) The dynamic fracture toughness of Chevron-notch alumina specimens were 17~20% higher than static ones, which is higher difference than 10% in the brittle cast irons. This study showed that the proposed dynamic fracture toughness measuring method using Chevron -notch specimen is valid in both static and dynamic modes.

## Acknowledgements

This study was financially supported by Chonnam National University in the year of 1998.

## References

1. R.W. Davidge and G. Tappin, In Proceedings of the British Ceramic Society, Vol. 15, pp. 47-60, 1970.
2. Nobuki Miyahara, Yoshiharru Mutoh, Kohich Tanaka and Manabu Takahashi, "Fracture Toughness Evaluation of Five Structural Ceramic Materilas by Various Testing Methods," Transactions of the Japan Society of Mechanical Engineers (A), Vol. 57, No. 538, pp. 1326-1333, 1991.
3. ASM Handbook Committee, ASM Handbook Volume 8 Mechanical Testing, ASM international, pp. 382-386, 1992.
4. T. L. Anderson, Fracture Mechanics 2nd ed., pp. 50-55, pp. 451-454, 1995.
5. Weinong Chen, and G. Ravinchandran, "Dynamic compressive failure of a glass ceramic under lateral confinement," J. Mech. Phys. Solids, Vol. 45, No.8, pp. 1303-1328A, 1997.
6. Richard J. Anton, and Ghatu Subhash, "Dynamic Vickers indentation of brittle materials," Wear, Vol. 239, pp. 23-35, 2000.
7. Beech, J. F., and Ingraffea, A. R., "Three -Dimensional Finite Element Calibration of The Short Rod Specimen, International Journal of Fracture," Vol. 18, pp. 217-229, 1982.
8. Raju, I. S., and Newman, J. C. Jr., " Three-Dimensional Finite-Element Analysis of The Chevron Notched Fracture Specimen," Technical Memorandum 85798, NASA Langley Research Center, April 1984.
9. Anthony R. Ingraffea, "Stress-Intensity Factor Computation in Three Dimensions with Quarter-Point Elements," International Journal for Numerical Methods In Engineering, Vol. 15, pp. 1427-1445, 1980.
10. M. H. Aliabadi and D. P. Rooke, Numerical Fracture

Mechanics, Computational Mechanics Pub., 1991.
11. J. Lankford, Journal of Material Science Letter, Vol. 1, pp. 493-495, 1982.